Hindawi
International Journal of Antennas and Propagation
Volume 2022, Article ID 8615436, 10 pages
https://doi.org/10.1155/2022/8615436

Research Article

Remote Calibration Technology in Target RCS Time Domain Outfield Measurement

Ming-Hao Gong,[1,2] Yi-Wen Li,[3] Bing Wei ,[1,2] and Xiao-Long Wei[3]

[1]*School of Physics, Xidian University, Xi'an 710071, China*
[2]*Collaborative Innovation Center of Information Sensing and Understanding at Xidian University, Xi'an 710071, China*
[3]*Science and Technology on Plasma Dynamic Laboratory, Airforce Engineering University, Xi'an 710038, China*

Correspondence should be addressed to Bing Wei; bwei@xidian.edu.cn

Received 3 June 2022; Revised 18 November 2022; Accepted 24 November 2022; Published 14 December 2022

Academic Editor: Ravi Gangwar

In this paper, a new method of remote calibration in time domain measurement of outfield RCS is proposed. Based on the basic principle of RCS time domain measurement and the characteristics of time domain system, the difference in time and frequency domain measurement is analyzed. The frequency domain remote calibration formula is extended to the time domain by time-frequency transform. Through the analysis of the time domain echo signal of the calibration body in the correction formula and the experimental verification of the calibration sphere echo signal, the influence of the calibration body size and measurement distance on the time domain echo signal and spectrum of the calibration body is given. The typical targets are measured by using the time domain system, and the results of time domain remote calibration, theoretical simulation, and frequency domain measurement are compared. The results show that the error between the time domain remote calibration results and the theoretical simulation results is not more than 1 dB at the −25 dB level. In the outfield measurement, this scheme can fully reflect the advantages of time domain measurement of wide frequency bands and low environmental requirements.

1. Introduction

Radar cross-section (RCS) measurement is one of the important ways to accurately understand the electromagnetic scattering characteristics of complex targets [1]. It has important applications in target identification and classification, imaging, radar countermeasures, stealth design, etc. [2–4]. Target RCS measurement methods include microwave anechoic chamber measurement in time-frequency domain and standard field measurement in the time-frequency domain [5–7]. The frequency domain RCS measurement method is relatively perfect in several decades of research. With the development of ultra-wide-band pulse power technology, ultra-wide-band antenna technology, and data acquisition technology [8–10], time domain measurement technology has been widely applied in imaging and electromagnetic interference (EMI) measurement due to its broadband characteristics and good time-space resolution [11–13]. Time domain narrow pulse RCS measurement technology is also attracting more and more attention. References [14, 15] describe the principle of electromagnetic scattering measurement using time domain tools and the RCS of typical targets. The time domain response of UWB radar signals from scattering targets is analyzed in [16]. The time domain description of the general scattering process is described mathematically. However, the measurement frequency band is lower than 1 GHz and the influence of environment and calibration volume in the actual measurement process is not discussed.

In RCS measurement, calibration is a key issue. It can be divided into relative calibration and absolute calibration [17]. At present, the research of calibration theory mainly focuses on the relative calibration method [18, 19]. To establish a strict correspondence between the known RCS and the physical quantity (voltage or power) output by the radar receiver, the RCS value of the unknown target can be

obtained from the measured value of the receiver. Therefore, it is necessary to accurately measure the echo signal of the calibration body and calculate its theoretical value [20]. The measurement scheme adopted in the research is mainly the frequency sweep of the external field, focusing on the selection of the calibration body and the analysis of errors [21–25]. However, the research literature and measurement related to RCS time domain measurement are mainly carried out in the anechoic chamber, and the research mainly focuses on radar link analysis and simulation [26–28]. The research on field measurement is less, and the relevant theoretical and experimental research on the calibration scheme in field measurement is even less. When the distance between the field measurement and the target measurement is far away, the acquisition scheme and accuracy of the signal received by the standard body have not been discussed yet.

In this paper, a new method of remote calibration in field RCS time domain measurement is presented. Firstly, the basic principle of RCS measurement in time domain and its difference with frequency domain measurement are analyzed. Based on the principle of frequency domain horizontal field remote calibration, the measurement correction equation of time domain remote calibration is derived. Then, through experimental measurement and theoretical analysis, the influence of calibration parameters such as size and measurement distance on the echo signal and spectrum of the calibration body in time domain external field measurement is studied. Finally, the time domain RCS measurement system was used to carry out a typical target RCS remote measurement experiment. The results show that the error between the time domain remote calibration results and the theoretical simulation results is not more than 1 dB at the −25 dB level. In the field measurement, this scheme can fully reflect the advantages of time-domain measurement of wide frequency bands and low environmental requirements.

2. RCS Time Domain Measurement Principle and System

2.1. RCS Time Domain Measurement Principle. In electromagnetic scattering, the mathematical expression of RCS is shown as follows [1]:

$$\sigma\left(\varphi_i, \theta_i; \varphi_s, \theta_s\right) = \lim_{\mathbf{r}\longrightarrow\infty}\left(4\pi\mathbf{R}^2\frac{\left|\mathbf{E}_s\right|^2}{\left|\mathbf{E}_i\right|^2}\right)\mathrm{sm}, \tag{1}$$

where $\mathbf{R}$ is the distance from the target to the radar, $\mathbf{E_i}$ and $\mathbf{E_s}$ are the intensity of incident and scattering electric fields, respectively, (φ_i, θ_i) is the direction of incident wave, and (φ_s, θ_s) is the direction of scattering observed. When the observation direction of the scattered field is opposite to the direction of the incident field, the radar cross section is called the single-station RCS. Through the derivation of the radar equation, the RCS definition can be transformed into the following [15]:

$$\begin{aligned}\sigma &= \xi \cdot P_r,\\ \xi &= 4\pi\frac{1}{P_tG_t}\frac{1}{G_r\lambda_0^2/\left(4\pi R^2\right)^2}\cdot L,\end{aligned} \tag{2}$$

where P_t and P_r are the transmitting power and receiving power of radar, respectively; G_t and G_r are the gains of transmitting antenna and receiving antenna, respectively; R is the distance from the transceiver antenna to the target; λ_0 is the wavelength of electromagnetic wave, L is the comprehensive influence of various losses in propagation.

In actual RCS measurement, if the measurement environment and conditions are guaranteed to be consistent, ξ can be approximately considered unchanged, and then [15],

$$\begin{aligned}\sigma_1 &= \xi \cdot \mathbf{P_{r1}}\sigma_2 = \xi \cdot \mathbf{P_{r2}},\\ \sigma_2 &= \frac{P_{r2}}{P_{r1}}\sigma_1 = \frac{\left|\mathbf{E_{r2}}\right|^2}{\left|\mathbf{E_{r1}}\right|^2}\sigma_1,\end{aligned} \tag{3}$$

where $\mathbf{E_{r1}}$ and $\mathbf{E_{r2}}$ are the scattered signal intensity of target 1 and target 2, respectively. If target 1 is a standard model, its theoretical value σ_1 can be obtained directly by numerical calculation.

RCS time domain measurement is used to measure the scattering characteristics of the target by using narrow pulse and ultra-wide-band (UWB) radar [6]. Among them, the narrow pulse in time domain is used as the excitation source, the ultra-wide-band radar is used as the transceiver, and the oscilloscope receives the time-domain scattering signal of the target. For the time domain measurement system, the received signal is the time domain pulse waveform that shows the real-time echo position and strength of the target. The RCS result of the measured target can be obtained by transforming it into the frequency domain representation through Fourier transform. If the time domain signal is represented as $f(t)$, its spectrum can be expressed as [29]

$$F(\omega) = \mathrm{FFT}\left[f(t)\right] = \int_{-\infty}^{\infty} f(t)e^{-\mathrm{iwt}}\mathrm{d}t. \tag{4}$$

The time domain expression of the target RCS to be tested is

$$\sigma_2(\theta, f) = \sigma_1(\theta, f)\cdot\left|FFT\left[\mathbf{E_{r2}}(\theta, t)\right]\right|^2/\left|FFT\left[\mathbf{E_{r1}}(\theta, t)\right]\right|^2, \tag{5}$$

where θ is the azimuth angle, $\mathbf{E_{r1}}(\theta, t)$ and $\mathbf{E_{r1}}(\theta, t)$ are the time domain responses of the calibration body and the target at the same position, respectively; $\sigma_1(\theta, f)$ and $\sigma_2(\theta, f)$ are functions of azimuth angle and frequency, respectively.

The common unit of RCS is m^2. After expressing equation (5) in decibels, equation (6) can be obtained as follows:

$$\begin{aligned}\sigma_2(\mathrm{dB\,sm}) = {}& 10\log\left[\left|FFT\left[\mathbf{E_{r2}}(\theta, t)\right]\right|^2\right]\\ & - 10\log\left[\left|FFT\left[\mathbf{E_{r1}}(\theta, t)\right]\right|^2\right] + 10\log\sigma_1.\end{aligned} \tag{6}$$

In RCS time domain measurement, it is necessary to measure the time domain echo response of all angles when no target is placed and the target is placed by rotating the low-scattering bracket through the stepped axis. Then, the time domain response of the calibration body in the same state is measured and its theoretical RCS is calculated. Finally, the RCS of all azimuth angles of target to be measured can be obtained by post-processing the data. Therefore, the accuracy of time domain measurement mainly depends on the accuracy of target time domain echo signal.

2.2. RCS Time Domain Measurement System. The RCS time domain measurement system consists of software and hardware. The system software is mainly used to display real-time signals, set measurement parameters, calibrate and process signals through programming, and display, record, and output measurement results. The hardware block diagram of the system is shown in Figure 1. The working principle is as follows: the time domain pulse excitation is provided by the pulse source; the scattering field of target is generated under the irradiation of incident plane wave (far-field approximation); the receiving antenna receives the target scattering field and passes the sampling receiver synchronized with the signal source to obtain the real-time scattering signal of the target; after data processing and analysis, the broadband electromagnetic characteristics of the target are obtained. The measurement accuracy and measurement range of the time domain system are determined by the system hardware parameters. For the pulse provided by the time domain pulse source, the higher the amplitude and the narrower the width of the pulse, the wider the spectrum that can be covered after the Fourier transform, and the higher the requirement for the accuracy and bandwidth of oscilloscope data acquisition. Due to the relatively low signal-to-noise ratio (SNR) and bandwidth of real-time oscilloscope, sampling oscilloscope is used in RCS time domain measurements. Sampling oscilloscope requires strict synchronization between the acquisition trigger signal and scattering echo signal. Therefore, the synchronous trigger signal is directly provided by the pulse source. Meanwhile, the spectrum of the incident wave is related to the transceiver antenna. In order to match the pulse source, the transceiver antenna adapts the same type of time domain ultra-wide-band antenna.

The time domain pulse source and equivalent sampling receiver used in the time domain system in this article are provided by GEOZONDAS. The time domain pulse waveform generated by the pulse source and its Fourier transform spectrum are shown in Figure 2. The time domain signal amplitude is 25 V, the full width at half maxima (FWHM) is less than (30 ± 2) ps, the maximum repetition frequency is 1 MHz, and the output pulse jitter is less than 2.5 ps. The energy of pulse is different at different frequencies, and the power of all frequency points is higher than 45 dBm in the range of 2–18 GHz. The high-precision sampling receiver SD203TMS synchronized with the pulse source adopts equivalent sampling technology. It records and saves the signals received by the antenna and cooperates with the software function to obtain the target's time domain and frequency domain response data. The receiver bandwidth is 0.1–26 GHz, the sampling rate is 1 MHz, the root mean squared (RMS) noise factor is −60 dB, the minimum time axis length is 0.02 ns, and the maximum time axis sampling points is 4096.

The time domain measurement mainly adopts "time window" filtering and background cancellation technology to reduce the measurement errors. "Time window" filtering means to remove multipath effect and antenna coupling interference in the measurement environment by selecting the size of time window and moving the position of time window. The multiple reflection signals and interference signals are isolated from the time window, and only the target signal is retained in the measurement time window. For example, in Figure 1, signal 2 is included in the time window. For different research targets and measurement scenarios, the position and size of time window for echo signal extraction are different, which needs to be analyzed and tested according to the actual situation. Figure 3 shows the schematic diagram of time window selection in time domain measurement. Wherein, 0-$T1$ represents the time delay of the time domain measurement system, which is a constant value for the equipment stabilization system; $T1$-$T2$ indicates the main region of antenna coupling signal. The duration of the coupled signal lasts for a long time, but it gradually decreases with time, which reduces the impact on the target signal; $T2$-$T3$ represents the time difference between the antenna coupling signal and the target main echo signal. $T3$ can be estimated by measuring the distance between the transceiver antenna and the target; $T3$-$T4$ represents the target direct echo signal region, and the echo signal duration is calculated from the target size and approximate exposure range of the system plane wave; $T5$-$T6$ represents the background echo signal, which lags behind the direct main signal in time due to its long path. In time domain measurement, time window is usually selected with $T3$ as the starting position and $T4$ as the cut-off position. In the actual measurement of target RCS, the appropriate time window can be selected by modeling the site and target.

Background cancellation refers to taking the environment echo without target as signal background and subtracting the background signal from the real-time signal received by the system as the target echo signal in measurement. Both of these techniques can effectively reduce the time domain measurement errors. However, there are still many errors that cannot be filtered and canceled in the actual measurement, such as: the coupled signal between the target and the scattering bracket and the signal jitter in the delay measurement. Therefore, in the time domain RCS measurement, it is also necessary to improve the signal accuracy through repeated measurement of echo signal at the same angle and to improve the system sensitivity through coherent averaging of data. The improvement degree is $10 \log N$, N is the average times. However, the average method will increase the measurement time, which needs to be selected according to the measurement accuracy requirements and measurement time.

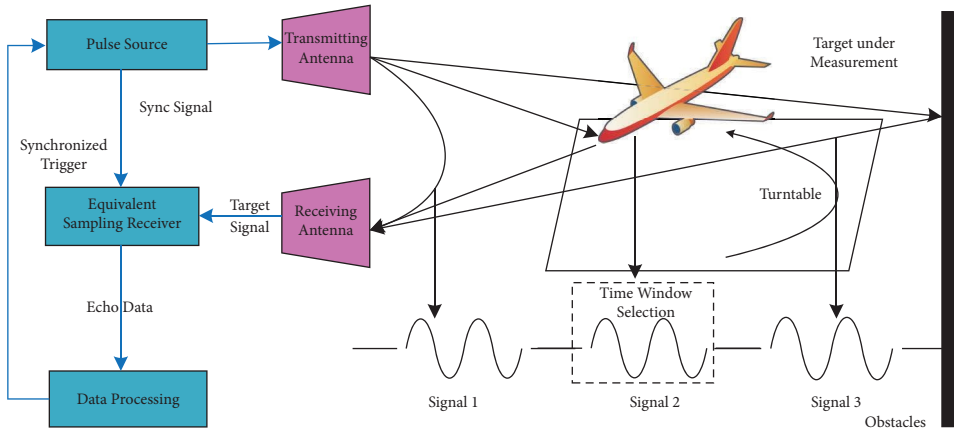

Figure 1: Time domain measurement system hardware block diagram.

2.3. RCS Time Domain Remote Calibration Principle. The RCS time domain measurement remote calibration equation is basically the same as the derivation process of the ground plane field remote calibration in the traditional frequency domain RCS measurement and is also derived from the simplified radar transmission equation [20]. When the same system is used to measure the target and the calibration body installed in different positions, the equation (3) can be rewritten as [21].

$$\sigma_2 = \xi_0 \cdot \frac{P_{r2}}{P_{r1}} \cdot \sigma_1 = \xi_0 \cdot \left|\frac{\mathbf{E_{r2}}}{\mathbf{E_{r1}}}\right|^2 \cdot \sigma_1. \tag{7}$$

In the equation, ξ_0 is the calibration constant. According to equation (2),

$$\xi_0 = (R_t/R_c)^4 \cdot (L_t/L_c), \tag{8}$$

where R_t and R_c are the distances from target and the calibration body to the radar, espectively; L_t and L_c are the total loss caused by system and atmospheric transmission in the measurement of target and calibration body, respectively. It is worth noting that the influence of various factors such as background clutter is ignored during the measurement.

In addition, in the remote calibration, it is also necessary to consider the influence caused by the difference between the target and the calibration body transmitting power P_m in the test field and their transmitting echo power P_r in free space, namely,

$$\frac{P_m}{P_r} = \frac{\left|\mathbf{E_m}\right|^2}{\left|\mathbf{E_r}\right|^2} = \xi, \tag{9}$$

where ξ is called the multipath gain factor generated by the geometric relationship of the test field and the antenna directivity. In actual measurement, due to the different placement positions of the calibration body and the target, the multipath gain factor at the calibration body ξ_2 is usually not completely consistent with the multipath gain factor at the target ξ_1. Therefore, under the condition of remote measurement, the relationship between target RCS and calibration body RCS is

$$\begin{aligned}\sigma_2 &= \frac{P_{m2}/\xi_2}{P_{m1}/\xi_1} \cdot \left(\frac{R_t}{R_c}\right)^4 \cdot \frac{L_t}{L_c} \cdot \sigma_1 \\ &= \frac{\left|\mathbf{E_{m2}}\right|^2}{\left|\mathbf{E_{m1}}\right|^2} \cdot \frac{\xi_1}{\xi_2} \cdot \left(\frac{R_t}{R_c}\right)^4 \cdot \frac{L_t}{L_c} \cdot \sigma_1,\end{aligned} \tag{10}$$

where the target echo intensity $\mathbf{E_{m2}}$ and the calibration body echo intensity $\mathbf{E_{m1}}$ received by the radar under remote conditions are measured known quantities; for the same system, $(R_t/R_c)^4$ is only related to the position of target and calibration body; L_t/L_c is only needed to calculate the atmospheric transmission loss; only the multipath gain factor term ξ_1/ξ_2 is difficult to estimate accurately.

In RCS time domain measurement, the multipath interference term ξ_1/ξ_2 can be reduced by the limitation of the transmit and receive antenna beam width and the high range resolution of ps-level narrow pulses. In the current application range of the time domain system, after a reasonable time window is selected, the influence of the multipath term in equation (10) is not considered for the moment. In the case of only considering the atmospheric transmission loss term L_t/L_c and the off-site distance term $(R_t/R_c)^4$, the time domain remote calibration equation is

$$\begin{aligned}\sigma_2\,(\mathrm{dB\,sm}) &= 10\log\left[\left|\mathrm{FFT}\left[\mathbf{E_{m2}}(\theta,\mathbf{t})\right]\right|^2\right] \\ &\quad - 10\log\left[\left|\mathrm{FFT}\left[\mathbf{E_{m1}}(\theta,\mathbf{t})\right]\right|^2\right] + 10\log\sigma_1 \\ &= 10\log\left[\left|\mathrm{FFT}\left[\mathbf{E_{m2}}(\theta,\mathbf{t})\right]\right|^2\right] + 10\log\sigma_1 \\ &\quad - 10\log\left[\left|\mathrm{FFT}\left[\mathbf{E'_{m1}}(\theta,\mathbf{t})\right]\right|^2\right] + 10\log\left[\left(\frac{R_t}{R_c}\right)^4 \cdot \frac{L_t}{L_c}\right].\end{aligned} \tag{11}$$

In the equation, $\mathbf{E_{m1}}(\theta,t)$ and $\mathbf{E_{m2}}(\theta,t)$ are, respectively, the time domain responses of the calibration body and target at the same location, and $\mathbf{E'_{m1}}(\theta,t)$ represents the time domain response of the calibration body when the calibration body and the target are in different places. The core idea of RCS time domain remote measurement is to correct the spectrum of echo signals at different distances from the

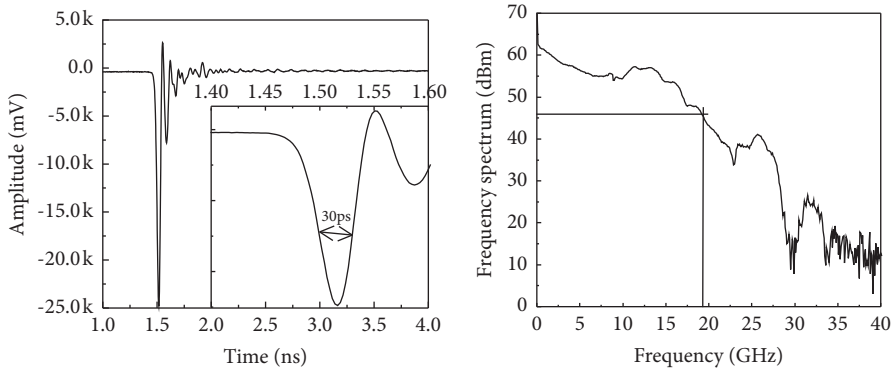

Figure 2: Pulse source time domain waveform and frequency spectrum. (a) Time domain pulse waveform and (b) pulse spectrum.

calibration body. Equation (11) is verified by comparing the analysis of the time domain echo signals of the calibration volume under the conditions of different sizes and distances and the RCS measurement results of typical targets.

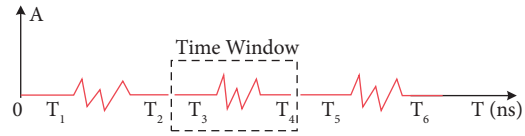

Figure 3: Schematic diagram of time window selection.

3. Experimental Results and Analysis

3.1. Time Domain Echo Signal Analysis of Calibration Sphere. As one of the most widely used RCS scales, metal spheres have the main advantage that the theoretical value of RCS can be simply calculated by MIE series expansion [1]. RCS is not affected by attitude angle, and it is relatively easy to manufacture. Therefore, metal spheres were selected as the calibration body for remote calibration in the measurement in this paper, and the feasibility of time domain remote calibration was verified by comparing the time domain pulse echo signal and its spectrum under different sizes and backgrounds. Figure 4 is the physical picture of metal spheres with different sizes.

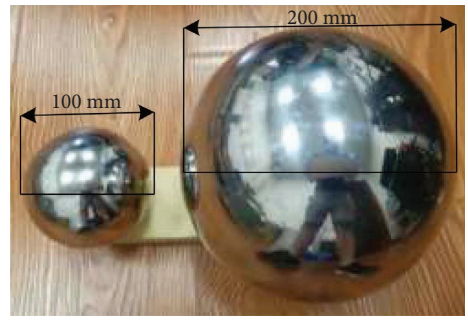

Figure 4: The physical map of the calibration sphere.

Figure 5 shows the echo responses of the calibration sphere after "time window" filtering and background cancellation under different conditions. Figure 5(a) shows the comparison of the echoes of calibration spheres of different sizes when the spherical center is 3.0 m away from the radar. Figure 5(b) is a comparison of echoes of a 200 mm diameter calibration sphere at different distances of the spherical center distance radar. As can be seen from Figure 5, the echoes of the calibration spheres of different sizes and distances have the same echo characteristics, and the main energy of the echo signal is concentrated in the range of 1 ns in the main echo region. The research [28, 29] shows that the horn antenna produces differential effect when radiating pulse signals. The calibration sphere signal received by the transceiver antenna in the system should be the second order differential of the pulse source signal. The calibration sphere echo in Figure 5 shows obvious second-order differential characteristics of the incident pulse under different conditions. At the same time, because the pulse source signal used in this system is a Gaussian-like pulse signal, there is obvious tailing and the influence of radio-frequency (RF) cable on the pulse shape cannot be completely ignored. Therefore, the differential waveform is distorted. Figure 6 shows the spectrum amplitude after the Fourier transform of the time domain signal at different distances from the 200 mm calibration sphere. The second order differential characteristics of the transceiver antenna to the incident pulse can also be seen from the spectrum characteristics.

Equation (11) can be used to calibrate the time domain echo signal and spectrum of the calibration ball at different distances, that is, the time domain signal of the calibration sphere at a distance of 2.0 m can be used to reversely deduce the time domain signal and spectrum of the same size calibration sphere at other distances. When the multipath effect is not considered, the calibration sphere time domain signal at the same distance as the target can be obtained in the case of remote measurement, and the target RCS can be calculated by equation (6).

3.2. Typical Target Experimental Results Analysis. In order to verify the effectiveness of the RCS remote calibration method, a typical target RCS measurement experiment was carried out using the time domain system. In the experiment, a metal sphere was used as the calibration body, and a

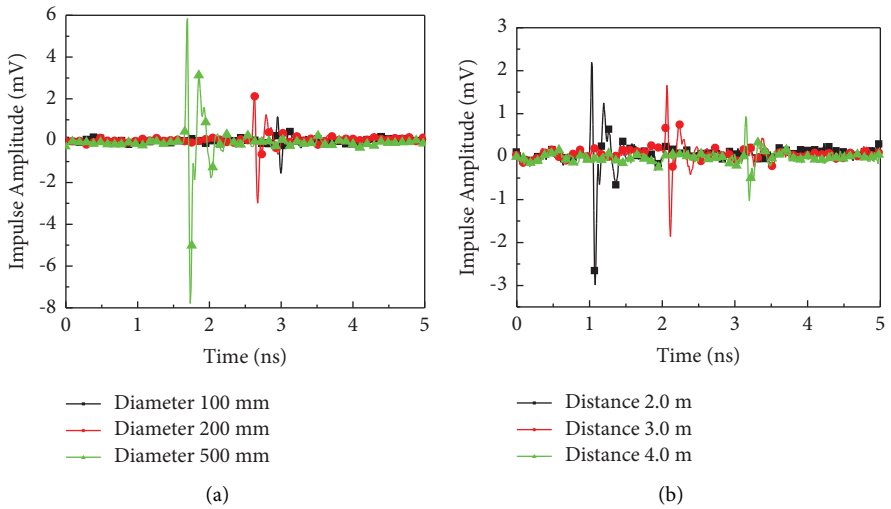

Figure 5: Time domain echo response of calibration sphere. (a) Time domain echo of different size calibration sphere and (b) time domain echo of calibration sphere at different distances.

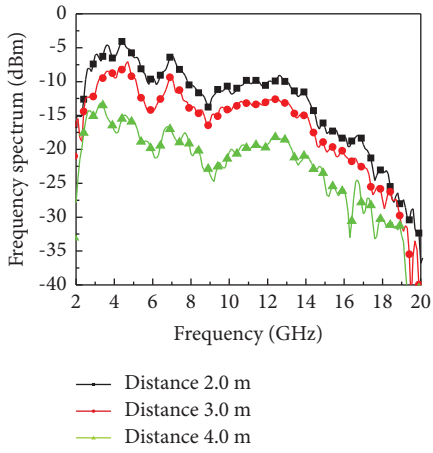

Figure 6: Spectral amplitude of calibration sphere echo.

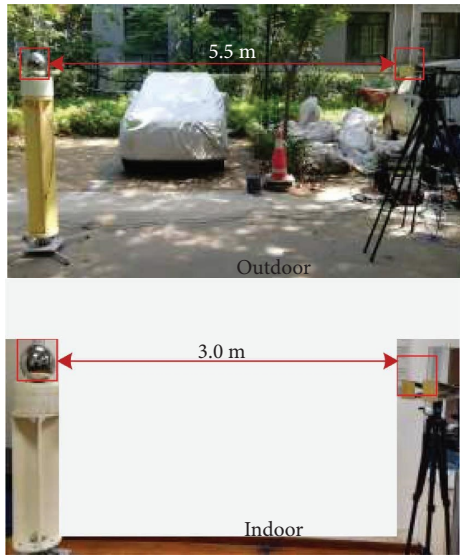

Figure 7: Calibration sphere time domain remote measurement chart.

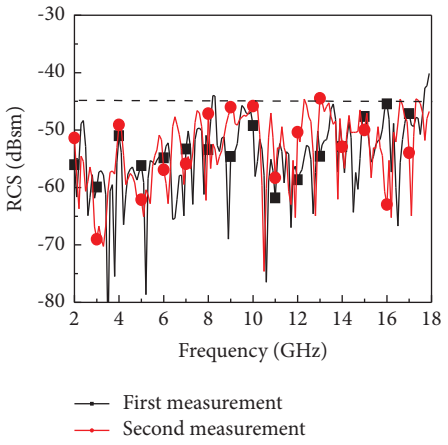

Figure 8: Background level RCS measurement results.

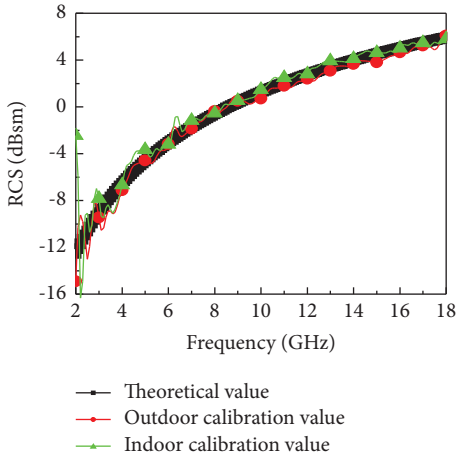

Figure 9: Metal plate RCS measurement results.

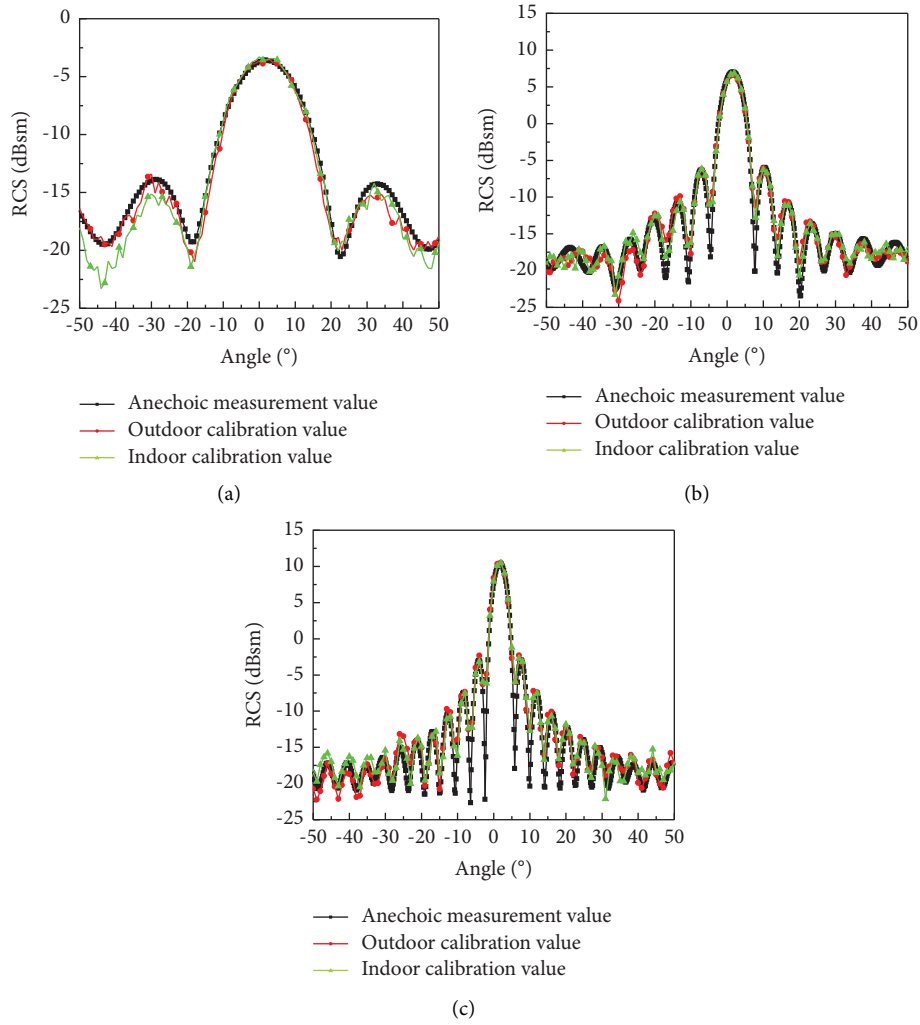

Figure 10: Graphite cube RCS measurement results. (a) Different angle RCS at 3 GHz, (b) different angle RCS at 10 GHz, (c) different angle RCS at 15 GHz.

metal plate and a graphite cube were used as the targets to be measured. The results of remote calibration of metal plate are compared with the on-site calibration and theoretical simulation results; and the results of different calibration of graphite cube are compared with the on-site calibration and frequency domain anechoic chamber measurements. The frequency band measured in this paper is 2–18 GHz. Therefore, the transmitter and receiver antennas in the time domain measurement system are selected as a double-ridged horn antenna with a bandwidth of 2–20 GHz, and the polarization mode is vertical polarization. Figure 7 shows the indoor and outdoor calibration scenes in this measurement. The time domain measurement process is consistent with the frequency domain measurement. In Experiment 1 and Experiment 2, the local calibration data were obtained by measuring the echo signals of the calibration sphere and the target to be measured simultaneously outdoors in the same place, and the remote calibration data were obtained by modifying the time domain echo signals of the indoor calibration sphere and the target to be measured outdoors. The received echo signal was coherently averaged 30 times in each measurement.

Experiment 1: Figures 8 and 9 show the RCS measurement results of a metal plate with a size of 10 cm × 10 cm. Figure 8 shows the measurement results of background level RCS in the outdoor field measurement. It can be seen that it is lower than −45 dB within the measurement frequency range, which meets the measurement requirements of the signal-to-noise ratio. Figure 9 shows the comparison of the theoretical value of the RCS of the metal plate with frequency when the electromagnetic wave is vertically incident on the surface of the metal plate and the measurement results in the two cases. The theoretical value is obtained through MATLAB simulation calculation, which is consistent with the reference [14]. The mean error between the measurement results and the theoretical value in the whole frequency band is less than 1 dB. The large error at the low frequency end is caused by the poor low frequency performance of the antenna and the scattering bracket, and the system time domain waveform is greatly interfered by the environment in the low frequency band. Compared with the

Table 1: RMS errors of the graphite cube measurement results at different frequencies.

	3 GHz	5.6 GHz	10 GHz	12.4 GHz	15 GHz
Indoor calibration	1.32 dB	1.21 dB	0.91 dB	0.54 dB	0.79 dB
Outdoor calibration	2.59 dB	1.56 dB	1.53 dB	1.42 dB	1.30 dB

Table 2: Compare the performance of different systems.

	Measuring environment	Calibration volume & calibration theory	Maximum measurement distance
Remote calibration system in paper	Free space	Simple	Tens of meters
Time domain system in [30]	Microwave anechoic chamber	Simple	Tens of meters
Frequency domain system in [25]	Wave-absorbing materials are needed	Complex	Several hundred meters

theoretical value, the root mean squared (RMS) error of indoor calibration is 0.54 dB, and the RMS error of outdoor calibration is 0.77 dB.

Experiment 2: RCS measurement of $20\,\text{cm} \times 20\,\text{cm} \times 20\,\text{cm}$ graphite cube. 3 GHz, 10 GHz, and 15 GHz were measured in the frequency domain darkroom by the point frequency measurement method. Figure 10 shows the comparison of the measurement results in the frequency domain anechoic chamber and the time domain at three frequency points. The frequency domain anechoic chamber results are obtained by using standard instruments in an authoritative measuring institution. The errors of the three methods at different angles are all less than 1 dB at high frequency and high level. The remote calibration error obviously increases at the low level of 3 GHz, which is considered to be due to the increasing multipath coupling interference that cannot be removed in the time domain echo signals received by the system in the same and remote calibration at low frequencies. Compared with the measurement results in frequency domain, the RMS errors of indoor calibration and outdoor calibration measurements in time domain at different frequencies are shown in Table 1. It can be seen from the table that the RMS error of outdoor calibration has a certain increase compared with that of indoor calibration. This is caused by the large interference of outdoor environment.

From the measurement results of two typical targets, it can be seen that it is feasible to extend the frequency domain off-site calibration theory to the time domain through time-frequency transformation. In time domain measurement, the time domain echoes at different positions of the calibration body can be modified into the calculation formula to obtain the accurate RCS of the target. The measurement results are consistent with the theoretical value or the measurement in frequency domain. However, the current measurement is mainly aimed at typical simple targets, and the measurement of complex targets requires further experiments. At the same time, due to the mutual limitation of measurement bandwidth and the transmission power of the pulse source in the current time domain system, the maximum measurement distance of the system is small. In frequency domain RCS measurement, the maximum measurement distance is usually determined by radar link budget analysis. However, in time domain measurement, because the waveform of its transmission signal source is fixed (the energy of signals at different frequencies in the measurement is different), the gain of the transceiver antenna at different frequencies is different. Therefore, when analyzing the maximum test distance through the radar link, the maximum distance that can receive the distinguishable target signal shall prevail. For the signal source and measurement system in this paper, we take the 200 mm metal ball in Figure 5(b) as an example. When it is 10 m away from the transceiver antenna, it is impossible to accurately obtain the target signal. Therefore, the maximum measurement distance (−30 dB) of the system is 10 m. The measurement does not take into account the error caused by dispersion effect, which needs further study.

4. Conclusion

Aiming at the problem that target the calibration body and cannot be measured simultaneously in RCS time domain measurement, a new method of time domain remote calibration is proposed. The equation of remote calibration using echo of the calibration body is derived by studying the theory of RCS time domain measurement and analyzing the target echo signal. The RCS measurement experiments of typical targets show that the RCS measurement technique based on radar equation and time domain echo analysis can be applied to the calibration in time domain field. As shown in Table 2, compared with the systems in other literature, the time domain system using the calibration theory in this paper can uses a simple calibration body to achieve target RCS measurement in the free space field.

This scheme can fully reflect the advantages of time-domain measurement of wide frequency band and low environmental requirements. It has certain practical value in engineering application.

Data Availability

The data used to support the findings of this study are included within the article.

Conflicts of Interest

The authors declare that they have no conflicts of interest.

Acknowledgments

This work was supported in part by the National Natural Science Foundation of China (61901324, 62001345, 62201411), in part by the Fundamental Research Funds for the Central Universities (XJS200501, XJS200507, JB200501, XJS222704), in part by the China Postdoctoral Science Foundation (2019M653548, 2019M663928XB).

References

[1] X. M. Pan and X. Q. Sheng, "Efficient wide-band evaluation of electromagnetic wave scattering from complex targets," *IEEE Transactions on Antennas and Propagation*, vol. 62, no. 8, pp. 4304–4313, 2014.

[2] M. Potgieter, J. W. Odendaal, C. Blaauw, and J. Joubert, "Bistatic RCS measurements of large targets in a compact range," *IEEE Transactions on Antennas and Propagation*, vol. 67, no. 4, pp. 2847–2852, 2019.

[3] Y. Q. Yang, C. M. Zhang, and A. E. Fathy, "Development and implementation of ultra-wideband see-through-wall imaging system based on sampling oscilloscope," *IEEE Antennas and Wireless Propagation Letters*, vol. 7, pp. 465–468, 2008.

[4] J. M. Geffrin, C. Eyraud, and A. Litman, "3-D Imaging of a microwave absorber sample from microwave scattered field measurements," *IEEE Microwave and Wireless Components Letters*, vol. 25, no. 7, pp. 472–474, 2015.

[5] J. M. Geffrin, C. Eyraud, A. Litman, and P. Sabouroux, "Optimization of a bistatic microwave scattering measurement setup: from high to low scattering targets," *Radio Science*, vol. 44, no. 2, pp. 1–12, 2009.

[6] B. Levitas, J. Matuzas, and M. Drozdov, "UWB Time Domain system for RCS measurements," in *Proceedings of the IEEE 13th International Radar Symposium*, pp. 241–244, Warsaw, Poland, May 2012.

[7] E. Pancera, T. Zwick, W. Wiesbeck et al., "Characterization of UWB Radar targets: time domain vs. frequency domain description," in *Proceedings of the IEEE Radar Conference*, pp. 1377–1380, Lecce, Italy, June 2010.

[8] C. X. Li, R. Z. Zhang, C. G. Yao et al., "Development and simulation of a compact picosecond pulse generator based on avalanche transistorized marx circuit and microstrip transmission theory," *IEEE Transactions on Plasma Science*, vol. 44, no. 10, pp. 1907–1913, 2016.

[9] S. F. Wang and Y. Z. Xie, "Far-field boundary estimation for the high-power UWB pulsed antennas," *IET Microwaves, Antennas & Propagation*, vol. 12, no. 14, pp. 2199–2205, 2018.

[10] K. Rambabu, A. E. C. Tan, K. K. M. Chan, and M. Y. W. Chia, "Estimation of antenna effect on ultra-wideband pulse shape in transmission and reception," *IEEE Transactions on Electromagnetic Compatibility*, vol. 51, no. 3, pp. 604–610, 2009.

[11] X. Z. Zeng, A. Fhager, M. Persson, and H. Zirath, "Performance evaluation of a time domain microwave system for medical diagnostics," *IEEE Transactions on Instrumentation and Measurement*, vol. 68, no. 8, pp. 2880–2889, 2019.

[12] S. Heunisch, L. O. Fhager, and L. E. Wernersson, "Millimeter-wave pulse radar scattering measurements on the human hand," *IEEE Antennas and Wireless Propagation Letters*, vol. 18, no. 7, pp. 1377–1380, 2019.

[13] H. H. Slim and P. Russer, "A time domain system for the measurement of non-stationary EMI up to 40 GHz," in *Proceedings of the IEEE 2012 Asia-Pacific Symposium on Electromagnetic Compatibility*, pp. 205–208, Singapore, May 2012.

[14] Y. Chevalier, Y. Imbs, B. BeiUard et al., "UWB measurements of canonical targets and RCS determination," in *Proceedings of the Ultra- Wideband Short-Pulse Electromagnetics 4 (IEEE Cat. No.98EX112)*, pp. 329–334, Springer, Boston, MA, June 1998.

[15] W. A. Van Cappellen, R. V. De Jongh, and L. P. Ligthart, "Potentials of ultra-short-pulse time domain scattering measurements," *IEEE Antennas and Propagation Magazine*, vol. 42, no. 4, pp. 35–45, 2000.

[16] E. Pancera, T. Zwick, and W. Wiesbeck, "Correlation properties of UWB Radar target impulse responses," in *Proceedings of the 2009 IEEE Radar Conference*, pp. 1–4, Pasadena, California, May 2009.

[17] C. J. Bradley, *The Calibration of Bistatic Radar Cross Section Measurement*, Air Force Institute of Technology Air University, America, 2001.

[18] G. Bernd, R. Horn, M. Limbach et al., "Calibration techniques for active RCS-targets," in *Proceedings of the IEEE 7th European Conference on Antennas and Propagation*, pp. 3127–3131, Gothenburg, Sweden, April 2013.

[19] C. Bradley, P. Collins, J. Fortuny-Guasch et al., "An investigation of bistatic calibration objects," *IEEE Transactions on Geoscience and Remote Sensing*, vol. 43, no. 10, pp. 2177–2184, 2005.

[20] S. F. Kang, D. B. Ge, Z. Z. Zhang et al., "Study on active absolute calibration technique of airborne backscattering measurement radar," in *Proceedings of the IEEE International Geoscience and Remote Sensing Symposium*, pp. 2209–2211, Toronto, ON, Canada, June 2002.

[21] P. F. Wu and X. J. Xu, "Error analysis of relative calibration for RCS measurement on ground plane range," *Journal of Radars*, vol. 1, no. 1, pp. 58–62, 2012.

[22] D. Hotte, R. Siragusa, Y. Duroc, and S. Tedjini, "Radar cross-section measurement in millimetre-wave for passive millimetre-wave identification tags," *IET Microwaves, Antennas & Propagation*, vol. 9, no. 15, pp. 1733–1739, 2015.

[23] M. Pienaar, J. W. Odendaal, J. Joubert, J. E. Cilliers, and J. C. Smit, "Active calibration target for bistatic radar cross-section measurements," *Radio Science*, vol. 51, no. 5, pp. 515–523, 2016.

[24] C. Blaauw, J. E. Cilliers, and M. Potgieter, "Review of a full-polarimetric calibration target for radar cross section measurements," in *Proceedings of the IEEE International Workshop on Computing, Electromagnetics, and Machine Intelligence*, pp. 25-26, Stellenbosch, South Africa, November 2018.

[25] P. F. Wu and X. J. Xu, "Improved calibration technique for quasi-monostatic polarimetric measurement system using a dihedral as the calibration reference," *IEEE Transactions on Antennas and Propagation*, vol. 67, no. 11, pp. 7040–7049, 2019.

[26] W. Sörgel and W. Wiesbeck, "Influence of the antennas on the ultra-wideband transmission," *EURASIP Journal on Applied Signal Processing*, vol. 2005, no. 3, pp. 843268–843305, 2005.
[27] K. Rambabu, A. E.-C. Tan, K. K. M. Chan, and M. Y. W Chia, "Experimental verification of link loss analysis for ultra-wideband systems," *IEEE Transactions on Antennas and Propagation*, vol. 59, no. 4, pp. 1428–1432, 2011.
[28] A. E. C. Tan, M. Y. W. Chia, K. K. M. Chan, and K. Rambabu, "Modeling the transient radiated and received pulses of ultra-wideband antennas," *IEEE Transactions on Antennas and Propagation*, vol. 61, no. 1, pp. 338–345, 2013.
[29] D. B. Ge and B. Wei, *Electromagnetic Wave Theory*, EMW Publishing Company, vol. 2, pp. 399–406, Kendall Square, Cambridge, 1rd edition, 2011.
[30] S. L. Li, X. X. Yin, L. Wang, H. Zhao, L. Liu, and M. Zhang, "Time domain characterization of short-pulse networks and antennas using signal space method," *IEEE Transactions on Antennas and Propagation*, vol. 62, no. 4, pp. 1862–1871, 2014.